HHS Public Access

Author manuscript

Alzheimers Dement. Author manuscript; available in PMC 2022 April 01.

Published in final edited form as:

Alzheimers Dement. 2021 April ; 17(4): 618–628. doi:10.1002/alz.12224.

Biphasic cortical macro and microstructural changes in autosomal dominant Alzheimer disease

Victor Montal, MSc[1,2], **Eduard Vilaplana, PhD**[1,2], **Jordi Pegueroles, MSc**[1,2], **Alex Bejanin, PhD**[1,2], **Daniel Alcolea, PhD**[1,2], **María Carmona-Iragui, PhD**[1,2,3], **Jordi Clarimón, PhD**[1,2], **Johannes Levin, PhD**[4,5], **Carlos Cruchaga, PhD**[6,7,8,9], **Neill R Graff-Radford, MD**[10], **James M Noble, MD**[11], **Jae-Hong Lee, MD**[12], **Ricardo Allegri, MD**[13], **Celeste M. Karch, PhD**[14], **Christoph Laske, MD**[15,16], **Peter Schofield, PhD**[17,18], **Stephen Salloway, MD**[19], **Beau Ances, MD**[6,7,9,20], **Tammie Benzinger, MD**[9,20], **Eric McDale, DO**[6,9], **Randall Bateman, MD**[6,7,9], **Rafael Blesa, PhD**[1,2], **Raquel Sánchez-Valle, PhD**[21], **Alberto Lleó, PhD**[1,2], **Juan Fortea, PhD**[1,2,3], **Dominantly Inherited Alzheimer Network (DIAN)**

[(1)]Sant Pau Memory Unit, Department of Neurology, Hospital de la Santa Creu i Sant Pau, Biomedical Research Institute Sant Pau, Universitat Autònoma de Barcelona, Barcelona, Spain.

[(2)]Center of Biomedical Investigation Network for Neurodegenerative Diseases (CIBERNED), Madrid, Spain

[(3)]Barcelona Down Medical Center. Fundació Catalana de Síndrome de Down. Barcelona, Spain.

[(4)]Department of Neurology, Ludwig-Maximilians-Universität München, Munich, Germany;

[(5)]German Center for Neurodegenerative Diseases; Munich Cluster for Systems Neurology (SyNergy), Munich, Germany

[(6)]Department of Neurology, Washington University School of Medicine, St Louis, MO, USA

[(7)]The Hope Center for Neurological Disorders, St Louis, MO, USA

[(8)]NeuroGenomics and Informatics, Washington University School of Medicine, St. Louis, MO, USA

[(9)]Knight Alzheimer's Disease Research Center, Washington University School of Medicine, St Louis, MO, USA

[(10)]Department of Neurology, Mayo Clinic, Jacksonville, FL, USA

[(11)]Department of Neurology, Taub Institute for Research on Alzheimer's Disease and the Aging Brain, Columbia University Irving Medical Center, New York, NY, USA

[(12)]Department of Neurology, University of Ulsan College of Medicine, Asan Medical Center, Seoul, Korea

[*]Corresponding author: Juan Fortea Ormaechea, Memory Unit, Department of Neurology, Hospital of Sant Pau. Sant Antoni María Claret, 167. 08025. Barcelona. Spain., Phone number: (34) 935565986. Fax: (34) 935565602. jfortea@santpau.cat.

Competing interests:

R.J.B. has received honoraria from Janssen and Pfizer as a speaker, and from Merck and Pfizer as an advisory board member. E.M. has received royalty payments for an educational program supported by Eli Lilly and as a member of a scientific advisory board for Eli Lilly. All other authors report no competing interests.

[13]Department of Cognitive Neurology, Institute for Neurological Research Fleni, BuenosAires, Argentina

[14]Department of Psychiatry, Washington University School of Medicine, Saint Lous, MO, USA

[15]German Center for Neurodegenerative Diseases (DZNE) Tübingen, Germany

[16]Section for Dementia Research, Hertie Institute for Clinical Brain Research and Department of Psychiatry and Psychotherapy, University of Tübingen, Germany

[17]Neuroscience Research Australia, Sydney, Australia.

[18]School of Medical Sciences, University of New South Wales, Sydney, Australia.

[19]Neurology and the Memory and Aging Program, Butler Hospital, Providence, RI, USA

[20]Department of Radiology, Washington University in St. Louis, St. Louis, MO, Missouri, USA

[21]Alzheimer's Disease and Other Cognitive Disorders Unit, Hospital Clínic, Fundació Clínic per a la Recerca Biomèdica, Institut d'Investigacions Biomèdiques August Pi i Sunyer (IDIBAPS), Universitat de Barcelona, Barcelona, Spain

Abstract

INTRODUCTION: A biphasic model for brain structural changes in preclinical Alzheimer Disease could reconcile some conflicting and paradoxical findings in observational studies and anti-amyloid clinical trials.

METHODS: In this study we tested this model fitting linear vs quadratic trajectories and computed the timing of the inflection points vertexwise of cortical thickness and cortical diffusivity–a novel marker of cortical microstructure–changes in 389 participants from the Dominantly Inherited Alzheimer's Network.

RESULTS: In early preclinical AD, between 20 to 15 years before estimated symptom onset, \we found increases in cortical thickness and decreases in cortical diffusivity followed by, cortical thinning and cortical diffusivity increases in later preclinical and symptomatic stages. The inflection points 16 to 19 years before estimated symptom onset are in agreement with the start of tau biomarker alterations.

DISCUSSION: These findings confirm a biphasic trajectory for brain structural changes and have direct implications when interpreting MRI measures in preventive AD clinical trials.

Keywords

Alzheimer's disease; autosomal-dominant Alzheimer's disease; cortical diffusivity; MRI; biphasic cortical changes; preclinical Alzheimer's disease

1. BACKGROUND

Alzheimer disease has a long preclinical phase in which multiple pathophysiological alterations coexist. Individuals who carry mutations in the Presenilin-1, Presenilin-2 or amyloid precursor protein genes are destined to develop symptomatic Alzheimeŕs disease. Although autosomal dominant Alzheimer disease (ADAD) is an etiologically distinct form

of Alzheimer disease (AD), it shares pathological features, and a similar clinical presentation, to sporadic Alzheimeŕs disease.[1,2] The Dominantly Inherited Alzheimer Network (DIAN) Observational Study evaluates mutation carriers with standardized clinical and cognitive testing, brain imaging, and biochemical biomarkers with the goal of determining the sequence of changes in pre-symptomatic carriers. It is thus a unique population in which to study the timing of events in Alzheimeŕs disease pathophysiology.[3–5]

We have recently proposed a biphasic model of cortical changes in the preclinical stage of sporadic AD based on cross-sectional[6–8] and longitudinal data.[9] In this model, early pathological cortical thickening in Alzheimeŕs disease vulnerable regions is found in subjects with pathological CSF amyloid levels and normal CSF tau levels. This phase, which might be due to early neuroinflammatory changes,[10] is followed by atrophy once CSF tau also becomes abnormal.[7–9,11,12] Several cross-sectional studies have analyzed the brain structural changes in ADAD showing different cortical changes at different preclinical stages. Cortical thinning occurs in the precuneus, and temporal lateral regions seven to three years prior to symptom onset.[3] However, in young presymptomatic mutation carriers increased cortical thickness[10,13–16] and increased volumes in subcortical regions[13,17,18] have been described in small cohorts of ADAD.

Diffusion tensor imaging enables the study of the brain microstructure. Most diffusion weighted imaging studies in AD have focused on the white matter. However, it can also be used to study the cortical microstructure.[13,19] Cortical mean diffusivity has been proposed as a new biomarker in neurodegenerative diseases that could be more sensitive than cortical thickness to detect cortical changes, especially on symptomatic phases of the disease.[8,13,19–21] Importantly, cortical mean diffusivity also follows a biphasic trajectory in sporadic AD, with early decreases associated with cortical thickening and increases in later preclinical phases.[8] Interestingly, previous small cohort studies of ADAD reported cortical mean diffusivity decreases in early presymptomatic ADAD[10,13,17] and later increases in symptomatic mutation carriers.[13,17]

Therefore, a biphasic trajectory of cortical changes might reconcile the aforementioned changes in ADAD (and sporadic Alzheimeŕs disease). However, this biphasic model is based on the comparison between the different stages of preclinical Alzheimeŕs disease,[8,9] or on observations in small ADAD studies.[10,13,17] It has not been mathematically tested. ADAD offers the opportunity to compare different mathematical models (ie. linear vs quadratic) to detect the inflection points at which these changes occur.

Using the largest sample of ADAD, the multicenter DIAN cohort, we aimed to confirm and test this biphasic model of cortical changes in preclinical AD. Specifically, (i) we explored the trajectories of cortical thickness and cortical mean diffusivity comparing mutation carriers and non-carriers in relation to estimated years to symptoms onset, (ii) compared the fit of a biphasic (or quadratic) model as opposed to the linear one and computed the inflection point for cortical changes, and (iii) assess the influence of CSF pTau in the relationship between cortical alterations and estimated years to symptoms onset. A better characterization of the trajectory of MRI structural changes in ADAD and the confirmation

and characterization of this biphasic model in ADAD would inform the use of MRI outcome in current anti-amyloid preventive trials and future anti-inflammatory trials.

2. METHODS

2.1 Participants

Individuals from families with mutations in the presenilin-1, presenilin-2 and amyloid precursor protein genes were recruited from 14 sites participating in the DIAN observational study. We included all participants who had genetic, clinical data and an available quality checked MRI from the 12th data-freeze. The period of recruitment was January 2009 to December 2017. Estimated years to expected symptoms onset was computed as the difference between the participant's current age and the mutation-specific expected age of clinical symptoms onset.[3,22]. All participants provided written informed consent. Local ethical approval was obtained at each participating DIAN site.

2.2 Structural and diffusion MRI

MRI acquisition parameters were based on the ADNI protocol. Briefly, all subjects underwent a 3 Tesla T1-weighted scan at resolution of 1.1 × 1.1 × 1.2 mm voxels. Scans with artifacts were excluded. Images were processed with Freesurfer 5.3 and normalized to a standard space and smoothed using a Gaussian kernel of 15mm for statistical analysis as commonly done in cortical thickness analyses. A final number of 389 subjects with correctly preprocessed T1w images were included. Diffusion weighted images were available for a subset of the participants (N=300) with one b=0 and 64 directions at b=1000 with an isotropic voxel size of 2.5mm. We excluded 11 subjects due to image artifacts. We computed cortical mean diffusivity using a surface-based in-house pipeline as previously reported.[8] Briefly, we computed a rigid-body registration between the b=0 and the 64 b=1000 volumes to correct for motion effects. After removing non-brain tissue, a tensor model was fitted using FSL's *dtifit* command, and we computed the mean diffusivity metric. We then coregistered the b=0 scan to the segmented T1w image. Eight additional subjects were excluded due to incorrect registration. We then sampled the mean diffusivity volume for each participant at the midpoint cortical ribbon and projected it to each individual surface, previously constructed by Freesurfer, in order to generate individual cortical mean diffusivity maps. Finally, cortical diffusivity maps were normalized a standard surface template (*fsaverage*) and smoothed using a 15mm kernel. A total number of 281 participants were finally included in the cortical mean diffusivity analyses.

2.3 Biochemical quantifications of pTau

A subset of 327 individuals also underwent a lumbar puncture. CSF sample collection and measurement in the DIAN cohort has been previously described[23]. Briefly, CSF pTau181 (further referred as pTau) was measured by immunoassay using Luminex bead-based multi-plexed xMAP technology (INNO-BIA AlzBio3, Innogenetics).

2.4 Statistical analysis

Demographics were compared using the non-parametric test Man-Whitney U test and the Fisher's exact test as implemented in the R statistical software.

We designed three independent, but interrelated analyses to specifically assess the biphasic model in ADAD, using EYO as a proxy of disease staging. We first performed an exploratory analysis to compare cortical thickness and cortical mean diffusivity between mutation carriers and non-carriers in 5-year intervals with respect estimated symptom onset (ranges from −25 to +5) computing the vertex-wise Cohen's d effect size maps in order to explore group differences. We then used a 2-class general linear model to identify regions with statistically significant differences, including sex and education as nuisance factors. To avoid false positives, we corrected the results with a cluster-sized based MonteCarlo simulation with 10,000 repeats as implemented in Freesurfer (familywise error [FWE], $p < 0.05$).

Second, we compared different mathematical models (ie. linear vs quadratic). We initially assessed the linear relationship between both neuroimaging metrics and age in non-carriers, finding a significant association in non-carriers (Suppl Fig 1). Therefore, in order to mitigate this age-related effect and model the changes in mutation carriers, we first normalized each mutation carrier individual map using a W-score approach.[24,25] We finally compared the linear model and, the linear model with the addition of a quadratic term of estimated years to symptoms' onset to the model at each surface vertex:

$$\text{Wscore-NI} \sim \text{EYO}\text{\^{}}2 + \text{EYO}$$

We applied the Akaike information criterion (AIC) to assess the improvement in the model with the inclusion of the quadratic term. Importantly, the AIC penalizes model complexity to avoid the risk of overfitting the data. Afterwards, we assessed the statistical significance of the quadratic model in those regions were the addition of the quadratic term improved the fitting. In addition, we computed interaction analyses to assess if the quadratic relationship of the imaging biomarkers with EYO were significantly stronger in the mutation carriers compared to the non carriers, using the following model at each vertex:

$$\text{NI} \sim \text{EYO}\text{\^{}}2*\text{MutationStatus} + \text{EYO} + \text{Sex}$$

Only those regions that survived multiple comparisons based on cluster-extension Monte Carlo simulations are shown (FWE, $p < 0.05$).

Then, to assess the inflection point for the cortical changes we fitted a second-order polynomial equation (i.e a parabola) and computed the first derivative of the polynomial in a vertex-wise basis. Of note, we only report the inflection points in those regions where the addition of the quadratic term improved the fitting of our data. The second-order polynomial fitting and the AIC metric were computed using the python packages *numpy*[26] and *statsmodels*[27], respectively.

Finally, we compared if the relationship between both imaging markers and EYO differed depending on the CSF pTau positivity status in asymptomatic mutation carriers. We computed a threshold of pTau positivity based on a ROC analyses comparing asymptomatic vs symptomatic mutation carriers, using the Youden's algorithm. This threshold was used to

categorize mutation carrier individuals into positive or negative pTau individuals. Then, we used a vertex-wise interaction model defined as:

$$\text{Wscore-NI} \sim \text{EYO}*\text{pTauStatus}$$

Only regions that survived multiple comparisons based on cluster-extension Monte Carlo simulations are shown (FWE, $p < 0.05$).

3. RESULTS

3.1 Participants

Table 1 summarizes the demographics and clinical data of all participants. There were no statistical differences in age, sex distribution, estimated years to symptoms onset or mutation type frequency between the mutation carriers and the non-carriers. As expected, we found significant differences in global CDR scores and CSF pTau measurements ($p < 0.001$).

3.2 Cortical macro and microstructural changes with respect estimated years to symptom onset

We first compared the cortical thickness and cortical mean diffusivity between carriers and non-carriers in 5-year age intervals (Figure 1 and Suppl Fig 2). The youngest mutation carriers (25 to 20 years before symptom onset) showed significant cortical thinning in middle temporal regions and increased diffusivity on the insula, with non-significant middle-to-high effect size differences in the precuneus and in the anterior cingulate and medial prefrontal cortex. Between 20 to 15 years before estimated symptom onset there was a shift, and mutation carriers showed significant increased cortical thickness in the occipital fusiform and insula and non-significant middle-to-high effect size in the precuneus, lateral temporal cortex, whereas mutation carriers showed significant reduced diffusivity on the left insula and frontal-parietal cortices and non-significant middle-to-high effect size differences posterior cingulate and lateral temporal regions. In the decade before symptom onset, mutation carriers showed significant cortical thinning in temporoparietal and occipital areas and increased cortical mean diffusivity in the precuneus and lateral and medial occipitotemporoparietal regions that further extended after the onset of clinical symptoms.

3.3 Cortical thickness and cortical diffusivity change following a quadratic model in preclinical AD

We then compared a quadratic vs a linear modeling for the normalized cortical changes (W-scores) in the mutation carriers individuals. Specifically, we first calculated if the addition of a quadratic term of EYO to the linear model at each surface vertex W-scores improved data fitting (Suppl Fig 3). Fig 2 (left panels) show the regions where the quadratic term of estimated years to onset for both neuroimaging metrics were significant after correcting for overfitting using the AIC criteria and correcting for multiple comparisons. The normalized cortical thickness (Fig 2 top row) showed a significant quadratic relationship in regions of the temporal cortex, temporoparietal junction, and parts of the precuneus and parieto-occipital regions. The normalized cortical mean diffusivity revealed a more widespread pattern of regions with significant quadratic relationships, especially in the lateral and

medial temporal cortex, the precuneus, and temporoparietal regions. Of note, the results are qualitatively the same when restricting the analyzing the PSEN1 carriers alone and when analyzing the PSEN2 and APP mutation carriers combined (results not shown). Moreover, when comparing mutation carriers against non carriers, we found that the relationship between each imaging marker and EYO^2 was significantly higher in the mutation carriers in regions typically described to be affected in AD (Suppl Figure 4).

3.4 Structural MRI markers inflection points are coincident with biochemical neurodegenerative biomarkers

We then calculated the inflection points for both the normalized cortical thickness and the normalized cortical mean diffusivity after fitting a second-order polynomial in the regions where the quadratic term was significant. To this aim, we computed the first derivative of the polynomial in a vertex-wise basis. Our data show that for cortical thickness, the trajectory changed around −18.8 years of onset and for cortical mean diffusivity around −16.25 years of onset. Of note, similar results were found when excluding the individuals with EYO>0 (Suppl. Fig 5).

3.5 The association between both cortical thickness and cortical mean diffusivity and estimated years to symptom onset depends on CSF pTau status

We dichotomized mutation carriers into pTau positive (pTau+) or negative (pTau−) using a threshold of 52.8 pg/ml, in order to run interaction analyses of the relationship between imaging markers and EYO by pTau status. Figure 3 shows the brain areas where/in which these interactions were significant. Specifically, we found a cluster of significant interaction for cortical thickness in parieto-occipital regions of the left hemisphere (Figure 3 top-row left panel) that was driven by increases of cortical thickness related to EYO in the pTau− and atrophy in the pTau+ (Figure 3 top-row right panel). For cortical mean diffusivity, we found a more widespread pattern of significant interactions, encompassing parieto-occipito-temporal areas bilaterally, and frontal regions for the right hemisphere (Figure 3 lower-row left panel). These interactions were driven by decreases of cortical diffusivity in relationship to EYO in the pTau− subgroup and diffusion increases in the pTau+ subgroup (Figure 3 top-row right panel).

3.6 A biphasic model of structural changes along the Alzheimer's Disease continuum

We finally integrate the proposed biphasic model for cortical macro and microstructural changes in relation with the reported pathophysiological biomarker changes in ADAD using the AT(N) framework[28] (Figure 4). Importantly, we did not categorize our individuals based on their biomarkers profiles, but contextualized the hypothetical biphasic model of alterations with previous findings in ADAD. Mutation carriers with EYO at the A−T− range present cortical thinning and increased cortical mean diffusivity. The onset of amyloid biomarker changes varies across ADAD studies, but between 25 to 20 years before estimated symptom onset, the rates of change in CSF Aβ42 values and amyloid uptake values start to occur.[29,30] This is 10 to 5 years before the earliest increases in CSF pTau levels have been reported.[31] Mutation carriers with EYO in the A+T− phase showed the first signs of increased cortical thickness and decreased cortical mean diffusivity changes in mutation carriers. The reported onset for CSF pTau increases is close to our calculated inflection

points for the trajectory of changes in both neuroimaging metrics. Thereafter, when comparing mutation carriers and non–carriers with EYO in the A+T_{CSF}+ phase, we did not see differences until the earliest reported alterations in tau PET, which occur 6 years before the symptoms onset[32]. When comparing individuals with EYO in this A+T_{PET}+ phase we found a widespread pattern of cortical thinning and increased cortical mean diffusivity. It is important to note that this biphasic trajectory does not occur in all the regions of the brain, but in specific regions. Furthermore, the temporality might vary in different areas of the cortex.

4. DISCUSSION

This study confirms that cortical thickness and cortical mean diffusivity follow a biphasic trajectory in ADAD. This model reconciles the apparently conflicting initial observations in small cohort studies. This biphasic trajectory should be considered when analyzing the MRI endpoints in preventive Alzheimeŕs disease clinical trials.

This study confirms initial observations from small ADAD cohorts, which had already reported cortical thickening and decreased cortical mean diffusivity in early preclinical AD in a small independent samples of presenilin-1 mutation carriers in Spain,[13–15] Colombia,[16] and Sweden.[10] Similarly, we and others have also reported increases of volume in subcortical structures.[13,17,18] Cortical mean diffusivity has also been assessed in a subset of the aforementioned studies. In agreement with our results, early decreases in cortical mean diffusivity were found in association with increased cortical thickness.[13] The present study not only confirms this early phase of cortical thickening, but importantly, it also shows, for the first time, that these changes are not neurodevelopmental, but pathological. Indeed, the youngest mutation carriers in the present study showed cortical thinning and increased cortical mean diffusivity. Cortical thickening and decreased mean diffusivity only emerged 20 to 15 years before estimated symptom onset. Atrophy, on the other hand, has been consistently reported in later preclinical (and symptomatic) ADAD. In this sense previous cross-sectional studies in DIAN and in other independent cohorts demonstrated cortical thinning in the precuneus ~7 to 4 years before symptom onset, a timing which is in agreement with our results.[3,33–36] Of note, although the main analyses show an overlapping pattern of changes for MD and CTh and between regions with the early increased cortical thickness and decreased cortical mean diffusivity and the later decreased cortical thickness and increased cortical mean diffusivity, some differences between modalities and regions should be further explored. We have previously shown that MD might have superior sensitivity than CTh[20], especially in frontal and insular regions. Furthermore, not all regions follow or are at the same pathophysiological stage in a given time-point[9], and some of the changes at early stages of the disease (co-occuring with presumably amyloid related inflammation as shown in a proof-of-concept deprenyl study in ADAD[10]) might not overlap completely with the later tau-related atrophy.

This paper provides the first mathematical modeling for a biphasic trajectory of changes in ADAD. The addition of a quadratic term significantly improved the linear model in several Alzheimer's disease vulnerable regions.[8,37] This analysis enabled us to calculate the inflection points for both the normalized cortical thickness and normalized cortical mean

diffusivity, which occurred 16 to 19 years before the expected symptom onset. This type of analyses can only be performed in ADAD, in which years to symptom onset can be reliably estimated. However, these analyses also require a large cohort of mutation carriers, which were not available in the aforementioned studies in the small independent ADAD cohorts. This biphasic trajectory of changes substantially expands the possibilities of MRI to detect the changes in preclinical Alzheimer's disease, if properly modeled. Indeed, it shows dynamic changes in the two decades prior to symptom onset as opposed to the aforementioned capability to detect atrophy in the last decade before symptom onset.

The interaction analyses showed clear differences when comparing the trajectories between CSF pTau+ and pTau− subgroups. In early preclinical Alzheimeŕs disease, in individuals with low CSF pTau values, cortical thickness increased and mean diffusivity decreased in mutation carriers, whereas in later stages, in those individuals with high CSF pTau values, there was cortical thinning and increases in cortical mean diffusivity. Interestingly, a previous longitudinal study in the DIAN cohort showed accelerated rates of atrophy up to 13 years before symptom onset in the precuneus,[30] earlier than the aforementioned cross-sectional studies. We speculate that longitudinal atrophy begins after CSF pTau levels start to increase, theoretically around 15 years before symptom onset (or earlier) in the DIAN cohort.[1,31] In this sense, we had previously shown that increased longitudinal atrophy rates can co-occur with increased cross-sectional cortical thickness.[14]

We finally integrate the cortical macro and microstructural changes in relation to the reported pathophysiological biomarker changes in ADAD. The timing of the cortical changes is strikingly congruent with those of amyloid and tau. The increase in cortical thickness and the decrease in cortical diffusivity coincided with the start of fibrillar amyloid accumulation,[15,30] around 20 years before symptom onset. However, 16 years before symptom onset, most regions had reached an inflection point, in agreement with the aforementioned reported increases in atrophy rates,[14,30] and the beginning of the increases in CSF pTau levels.[1,29,31] These results support the hypothesis previously reported by our group and others[8,9,38] that amyloid and tau have a toxic synergistic effect that might drive the inflexion point in cortical changes, leading to cortical atrophy and increases in cortical mean diffusivity. Finally, we found widespread cortical thinning and increased cortical mean diffusivity in subjects close to symptoms onset (EYO −5). Interestingly, this is the age-range at which the earliest increases in the uptake of tau PET have been reported.[32,39] Further work is needed in order to test the A/T/N framework in ADAD. This biphasic trajectory of changes is not unique to ADAD; our group and others have already shown early pathological cortical thickening and decreased cortical mean diffusivity in Alzheimer's disease vulnerable regions in cognitively unpaired subjects from the general population with pathological CSF Aβ42 levels and normal CSF tau levels.[8,40,41] Cortical thinning, and increases in mean diffusivity, only occurred in the presence of both abnormal amyloid and tau biomarkers.[6–9] The atrophy and increased mean diffusivity found in the youngest mutation carriers might reflect neurodevelopmental abnormalities. In this sense, in animal models using Tg2576 mice, decreased spine density and reduced levels of synaptophysin, in addition to behavioral changes have been described months prior to amyloid plaque deposition[42]. Similarly, in humans, Quiroz et al[43] reported cognitive vulnerabilities in verbal comprehension, processing speed and interpersonal relations tests, decades before the

symptom onset. However, further studies with larger sample sizes in this age-range and earlier time-points are needed to confirm this neurodebelopmental hypothesis. The rationale for cortical diffusivity decreases and cortical thickness increases early in AD has been previously reviewed.[10] In short, these changes could be related to amyloid-related inflammatory processes. Several studies have shown early astrocytic activation prior to neurodegeneration in animal models (see[44] for a review) and even prior to amyloid plaque accumulation in humans.[45] A local relationship has been demonstrated between astrocytosis measured using deprenyl PET and increases of cortical thickness and decreases of diffusivity in a Swedish ADAD cohort.[10]

Our results have important implications for the design of clinical trials with anti-amyloid therapies such as the Colombian (NCT01998841) and DIAN-TU (NCT01760005) cohorts. MRI measures are commonly used as endpoints, but under the assumption of a linear trajectory of changes. A biphasic trajectory in the design and interpretation of such trials outcomes should be considered. Our model might help understand the paradoxical findings in anti-amyloid trials (e.g. AN1792, solanezumab or bapineuzumab) where the active arm showed increased atrophy rates with respect to placebo (i.e a drug that effectively decreased amyloid related inflammation could lead to the counterintuitive effect of increasing atrophy, as it has been repeatedly shown in anti-amyloid trials). Our model also has immediate implications for secondary prevention trials in sporadic AD such as the A3 study (1R01AG054029–01), the A4 study (NCT02008357), ADAPT (NCT00007189) or TOMORROW (NCT01931566) trials as well as in future trials with anti-inflammatory drugs. Finally, this study confirms the sensitivity of cortical mean diffusivity to track the cortical microstructural changes in Alzheimeŕs disease.

The main strength of this study are the inclusion of the largest cohort of ADAD and the mathematical modeling of the biphasic trajectory using two complementary imaging measures. Our methodology to measure cortical mean diffusivity is another strength as it overcomes limitations previously reported when using voxel-based approaches, such as partial volume contamination and kernel-sensitive CSF inclusion during data smoothing.[46] Interestingly, cortical mean diffusivity captured the biphasic trajectory of changes in more widespread regions than cortical thickness. However, future studies should compare the sensitivity of cortical thickness and cortical mean diffusivity in the continuum of AD (both sporadic and ADAD), as it has been demonstrated in bvFTD[20]. This study also has several limitations. First, this study relies on the concept of estimated years to onset; however, several external factors might affect clinical presentation. Second, despite the use of a previously validated surface-based in-house pipeline developed to minimize CSF contamination, the cortical diffusivity might still be contaminated by partial volume effect related to the DWI low resolution. Finally, only a longitudinal study with long follow-ups periods with individual amyloid, tau, metabolic (PET-FDG) and inflammatory biomarkers will determine with accuracy the trajectory of changes at the individual level and the interplay between them. These analyses might become soon possible with the advent of plasma amyloid, tau and neurodegenerative biomarkers.

In summary, we showed that cortical changes in the preclinical ADAD follow a biphasic trajectory with early cortical thickening and decreases in cortical mean diffusivity followed

by atrophy and increases cortical mean diffusivity around 16 years before symptom onset, an age when CSF Tau levels start to increase. This biphasic trajectory might be crucial when interpreting MRI measures in current and future preventive trials in Alzheimer's disease.

Supplementary Material

Refer to Web version on PubMed Central for supplementary material.

Acknowledgments

We acknowledge the altruism of the participants and their families and contributions of the DIAN research and support staff at each of the participating sites for their contributions to this study. Data collection and sharing for this project was supported by The Dominantly Inherited Alzheimer's Network (DIAN, UF1AG032438) funded by the National Institute on Aging (NIA), the German Center for Neurodegenerative Diseases (DZNE), Raul Carrea Institute for Neurological Research (FLENI), Partial support by the Research and Development Grants for Dementia from Japan Agency for Medical Research and Development, AMED, and the Korea Health Technology R&D Project through the Korea Health Industry Development Institute (KHIDI).This manuscript has been reviewed by DIAN Study investigators for scientific content and consistency of data interpretation with previous DIAN Study publications. In addition, this project was founded by the Fondo de Investigaciones Sanitario (FIS), Instituto de Salud Carlos III (PI14/01126 and PI17/01019 to JF, PI13/01532 and PI16/01825 to RB, PI18/00335 to MCI, PI18/00435 to DA, PI14/1561 and PI17/01896 to A.L) and the CIBERNED program (Program 1, Alzheimer Disease to Alberto Lleó and SIGNAL study, www.signalstudy.es), partly jointly funded by Fondo Europeo de Desarrollo Regional, Unión Europea, Una manera de hacer Europa. This work was also supported by the National Institutes of Health (NIA grants 1R01AG056850 – 01A1; R21AG056974 and R01AG061566 to JF), Departament de Salut de la Generalitat de Catalunya, Pla Estratègic de Recerca i Innovació en Salut (SLT002/16/00408 to A.L), Fundació La Marató de TV3 (20141210 to JF, 044412 to RB); V. Montal is supported by Fondo de Investigaciones Sanitario (FI18/00275). This work was also supported by Generalitat de Catalunya (SLT006/17/00119 to JF, SLT006/17/95 to EV and SLT006/17/00125 to DA) and a grant from the Fundació Bancaria La Caixa to RB.

BIBLIOGRAPHY

1. Bateman RJ, Xiong C, Benzinger TLS, et al. Clinical and Biomarker Changes in Dominantly Inherited Alzheimer's Disease. N Engl J Med. 2012;367(9):795–804. doi:10.1056/NEJMoa1202753 [PubMed: 22784036]
2. Tang M, Ryman DC, McDade E, et al. Neurological manifestations of autosomal dominant familial Alzheimer's disease: a comparison of the published literature with the Dominantly Inherited Alzheimer Network observational study (DIAN-OBS). Lancet Neurol. 2016;15(13):1317–1325. doi:10.1016/S1474-4422(16)30229-0 [PubMed: 27777020]
3. Benzinger TLS, Blazey T, Jack CR, et al. Regional variability of imaging biomarkers in autosomal dominant Alzheimer's disease. Proc Natl Acad Sci U S A. 2013;110(47):E4502–9. doi:10.1073/pnas.1317918110 [PubMed: 24194552]
4. Reiman EM, Quiroz YT, Fleisher AS, et al. Brain abnormalities in young adults at genetic risk for autosomal dominant AD. Lancet Neurol. 2012;11(12):1048–1056. doi:10.1016/S1474-4422(12)70228-4.BRAIN [PubMed: 23137948]
5. Ridha BH, Barnes J, Bartlett JW, et al. Tracking atrophy progression in familial Alzheimer's disease: a serial MRI study. Lancet Neurol. 2006;5(10):828–834. doi:10.1016/S1474-4422(06)70550-6 [PubMed: 16987729]
6. Fortea J, Sala-Llonch R, Bartrés-Faz D, et al. Cognitively Preserved Subjects with Transitional Cerebrospinal Fluid ß-Amyloid 1–42 Values Have Thicker Cortex in Alzheimer Disease Vulnerable Areas. Biol Psychiatry. 2011;70(2):183–190. [PubMed: 21514924]
7. Fortea J, Vilaplana E, Alcolea D, et al. Cerebrospinal Fluid ß-Amyloid and Phospho-Tau Biomarker Interactions Affecting Brain Structure in Preclinical Alzheimer Disease. Ann Neurol. 2014;76(2):223–230. doi:10.1002/ana.24186 [PubMed: 24852682]
8. Montal V, Vilaplana E, Alcolea D, et al. Cortical microstructural changes along the Alzheimer's disease continuum. Alzheimer's Dement. 2017;(10):1–12. doi:10.1016/j.jalz.2017.09.013

9. Pegueroles J, Vilaplana E, Montal V, et al. Longitudinal brain structural changes in preclinical Alzheimer disease. Alzheimer's Dement. 2016;9(9):1–11. doi:10.1016/j.jalz.2016.08.010
10. Vilaplana E, Rodriguez-vieitez E, Ferreira D, et al. Cortical microstructural correlates of astrocytosis in autosomal- dominant Alzheimer ' s disease. Neurology. 2020;94:1:11.
11. Desikan RS, McEvoy LK, Thompson WK, et al. Amyloid-β associated volume loss occurs only in the presence of phospho-tau. Ann Neurol. 2011;70(4):657–661. doi:10.1002/ana.22509 [PubMed: 22002658]
12. Pascoal TA, Mathotaarachchi S, Mohades S, et al. Amyloid-β and hyperphosphorylated tau synergy drives metabolic decline in preclinical Alzheimer's disease. Mol Psychiatry. 2016;(10 2015):1–6. doi:10.1038/mp.2016.37 [PubMed: 26678307]
13. Fortea J, Sala-Llonch R, Bartrés-Faz D, et al. Increased cortical thickness and caudate volume precede atrophy in psen1 mutation carriers. J Alzheimer's Dis. 2010;22(3):909–922. doi:10.3233/JAD-2010-100678 [PubMed: 20858974]
14. Sala-Llonch R, Lladó A, Fortea J, et al. Evolving brain structural changes in PSEN1 mutation carriers. Neurobiol Aging. 2015;36(3):1261–1270. doi:10.1016/j.neurobiolaging.2014.12.022 [PubMed: 25638532]
15. Sala-Llonch R, Falgàs N, Bosch B, et al. Regional patterns of 18F-florbetaben uptake in presenilin 1 mutation carriers. Neurobiol Aging. 2019;81:1–8. doi:10.1016/j.neurobiolaging.2019.04.010 [PubMed: 31207465]
16. Quiroz YT, Schultz AP, Chen K, et al. Brain Imaging and Blood Biomarker Abnormalities in Children With Autosomal Dominant Alzheimer Disease. JAMA Neurol. 2015;02114:1–8. doi:10.1001/jamaneurol.2015.1099
17. Ryan NS, Keihaninejad S, Shakespeare TJ, et al. Magnetic resonance imaging evidence for presymptomatic change in thalamus and caudate in familial Alzheimer's disease. Brain. 2013;136(Pt 5):1399–1414. doi:10.1093/brain/awt065 [PubMed: 23539189]
18. Quan M, Zhao T, Tang Y, et al. Effects of gene mutation and disease progression on representative neural circuits in familial Alzheimer's disease. Alzheimers Res Ther. 2020;12(1):14. doi:10.1186/s13195-019-0572-2 [PubMed: 31937364]
19. Weston PSJ, Simpson IJA, Ryan NS, Ourselin S, Fox NC. Diffusion imaging changes in grey matter in Alzheimer ' s disease : a potential marker of early neurodegeneration. Alzheimers Res Ther. 2015;7(47):1–8. doi:10.1186/s13195-015-0132-3 [PubMed: 26584966]
20. Illán-Gala I, Montal V, Borrego-Écija S, et al. Cortical microstructure in the behavioural variant of frontotemporal dementia: looking beyond atrophy. Brain. 2019;142(4):1121–1133. doi:10.1093/brain/awz031 [PubMed: 30906945]
21. Vogt NM, Hunt JF, Adluru N, et al. Cortical Microstructural Alterations in Mild Cognitive Impairment and Alzheimer's Disease Dementia. Cereb Cortex. 12 2019:bhz286. doi:10.1093/cercor/bhz286
22. Ryman DC, Acosta-Baena N, Aisen PS, et al. Symptom onset in autosomal dominant Alzheimer disease: A systematic review and meta-analysis. Neurology. 2014;83(3):253–260. doi:10.1212/WNL.0000000000000596 [PubMed: 24928124]
23. Fagan AM, Xiong C, Jasielec MS, et al. Longitudinal Change in CSF Biomarkers in Autosomal-Dominant Alzheimer ' s Disease. 2014;6(226). doi:10.1126/scitranslmed.3007901
24. La Joie R, Perrotin A, Barre L, et al. Region-Specific Hierarchy between Atrophy, Hypometabolism, and -Amyloid (A) Load in Alzheimer's Disease Dementia. J Neurosci. 2012;32(46):16265–16273. doi:10.1523/JNEUROSCI.2170-12.2012 [PubMed: 23152610]
25. Bejanin A, La Joie R, Landeau B, et al. Distinct Interplay Between Atrophy and Hypometabolism in Alzheimer's Versus Semantic Dementia. Cereb Cortex. 2018;(5):1–11. doi:10.1093/cercor/bhy069 [PubMed: 29253248]
26. van der Walt S, Colbert SC, Varoquaux G. The NumPy Array: A Structure for Efficient Numerical Computation. Comput Sci Eng. 2011;13(2):22–30. doi:10.1109/MCSE.2011.37
27. Seabold S, Perktold J. statsmodels: Econometric and statistical modeling with python. In: 9th Python in Science Conference. ; 2010.

28. Jack CR, Bennett DA, Blennow K, et al. NIA-AA Research Framework: Toward a biological definition of Alzheimer's disease. Alzheimer's Dement. 2018;14(4):535–562. doi:10.1016/j.jalz.2018.02.018 [PubMed: 29653606]
29. McDade E, Wang G, Gordon BA, et al. Longitudinal cognitive and biomarker changes in dominantly inherited Alzheimer disease. Neurology. 2018:10.1212/WNL.0000000000006277. doi:10.1212/WNL.0000000000006277
30. Gordon BA, Blazey TM, Su Y, et al. Spatial patterns of neuroimaging biomarker change in individuals from families with autosomal dominant Alzheimer's disease: a longitudinal study. Lancet Neurol. 2018;17(3):211–212. doi:10.1016/S1474-4422(18)30028-0
31. Llibre-Guerra JJ, Li Y, Schindler SE, et al. Association of Longitudinal Changes in Cerebrospinal Fluid Total Tau and Phosphorylated Tau 181 and Brain Atrophy With Disease Progression in Patients With Alzheimer Disease. JAMA Netw open. 2019;2(12):e1917126. doi:10.1001/jamanetworkopen.2019.17126 [PubMed: 31825500]
32. Quiroz YT, Sperling RA, Norton DJ, et al. Association between amyloid and tau accumulation in young adults with autosomal dominant Alzheimer disease. JAMA Neurol. 2018;75(5):548–556. doi:10.1001/jamaneurol.2017.4907 [PubMed: 29435558]
33. Weston PSJ, Nicholas JM, Lehmann M, et al. Presymptomatic cortical thinning in familial Alzheimer disease: A longitudinal MRI study. Neurology. 2016;87(19):2050–2057. doi:10.1212/WNL.0000000000003322 [PubMed: 27733562]
34. Wang G, Coble D, McDade EM, et al. Staging biomarkers in preclinical autosomal dominant Alzheimer's disease by estimated years to symptom onset. Alzheimer's Dement. 2019;1:1–9. doi:10.1016/j.jalz.2018.12.008
35. Kinnunen KM, Cash DM, Poole T, et al. Presymptomatic atrophy in autosomal dominant Alzheimer's disease: A serial magnetic resonance imaging study. Alzheimer's Dement. 2018;14(1):43–53. doi:10.1016/j.jalz.2017.06.2268 [PubMed: 28738187]
36. Knight WD, Kim LG, Douiri A, Frost C, Rossor MN, Fox NC. Acceleration of cortical thinning in familial Alzheimer's disease. Neurobiol Aging. 2011;32(10):1765–1773. doi:10.1016/j.neurobiolaging.2009.11.013 [PubMed: 20005601]
37. Dickerson BC, Bakkour A, Salat DH, et al. The cortical signature of Alzheimer's disease: regionally specific cortical thinning relates to symptom severity in very mild to mild AD dementia and is detectable in asymptomatic amyloid-positive individuals. Cereb Cortex. 2009;19(3):497–510. doi:10.1093/cercor/bhn113 [PubMed: 18632739]
38. Pascoal TA, Mathotaarachchi S, Shin M, et al. Amyloid and tau signatures of brain metabolic decline in preclinical Alzheimer's disease. Eur J Nucl Med Mol Imaging. 2018:259–18. doi:10.1007/s00259-018-3933-3
39. Gordon BA, Blazey TM, Christensen J, et al. Tau PET in autosomal dominant Alzheimer's disease: relationship with cognition, dementia and other biomarkers. Brain. 2019. doi:10.1093/brain/awz019
40. Johnson SC, Christian BT, Okonkwo OC, et al. Amyloid burden and neural function in people at risk for Alzheimer's Disease. Neurobiol Aging. 2014;35(3):576–584. doi:10.1016/j.neurobiolaging.2013.09.028 [PubMed: 24269021]
41. Chételat G, Villemagne VL, Pike KE, et al. Larger temporal volume in elderly with high versus low beta-amyloid deposition. Brain. 2010;133(11):3349–3358. doi:10.1093/brain/awq187 [PubMed: 20739349]
42. Jacobsen SJ, Redwine JM, Morrison JH, et al. Early-onset behavioral and synaptic deficits in a mouse model of Alzheimer's disease. Proc Natl Acad Sci. 2006;103(13):5161–5166. doi:10.1073/pnas.0600948103 [PubMed: 16549764]
43. Quiroz YT, Pulsifer M, Chen K, et al. Cognitive Vulnerabilities in Presenilin-1 E280a Mutation-Carrying Children From the World'S Largest Autosomal-Dominant Alzheimer'S Disease Kindred. Alzheimer's Dement. 2017;13(7):P225–P226. doi:10.1016/j.jalz.2017.07.108
44. Drummond E, Wisniewski T. Alzheimer's disease: experimental models and reality. Acta Neuropathol. 2017;133(2):155–175. doi:10.1007/s00401-016-1662-x [PubMed: 28025715]

45. Rodriguez-Vieitez E, Saint-Aubert L, Carter SF, et al. Diverging longitudinal changes in astrocytosis and amyloid PET in autosomal dominant Alzheimer's disease. Brain. 2016:awv404. doi:10.1093/brain/awv404

46. Coalson TS, Van Essen DC, Glasser MF. The impact of traditional neuroimaging methods on the spatial localization of cortical areas. Proc Natl Acad Sci. 2018;115(27):E6356–E6365. doi:10.1073/pnas.1801582115 [PubMed: 29925602]

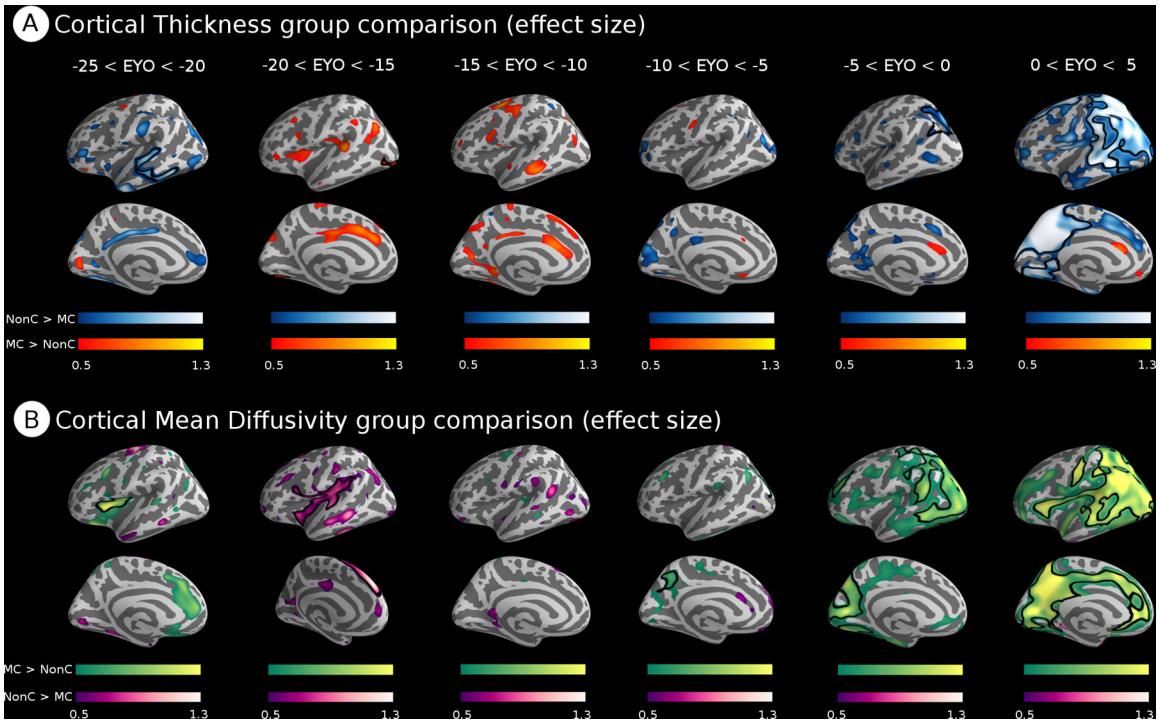

Figure 1. Group comparisons in cortical thickness and cortical mean diffusivity between carriers and non-carriers in 5-year age intervals.

We show the Cohen's d effect sizes to show trajectory of changes. Of note, only mid to high effect sizes are shown. Furthermore, statistically significant group differences clusters are outlined in black. For display purpose, only results in the left hemisphere are shown but the right hemisphere revealed similar changes. A) Cortical thickness effect size differences between the mutation carriers (MC) and the non-carriers (NonC) for different subsets of estimated years to onset. Blue is associated to less cortical thickness in the mutation carriers, whereas orange-yellow reflects higher cortical thickness in comparison to the non-carriers. B) Cortical mean diffusivity differences between mutation carriers and non-carriers for different subsets of estimated years to onset. Green is associated with increases of cortical mean diffusivity in the mutation carrier group, whereas purple reflects decreases in cortical mean diffusivity in comparison to the non-carriers. EYO = estimated years to onset; NonC = Non-carriers; MC = Mutation Carriers.

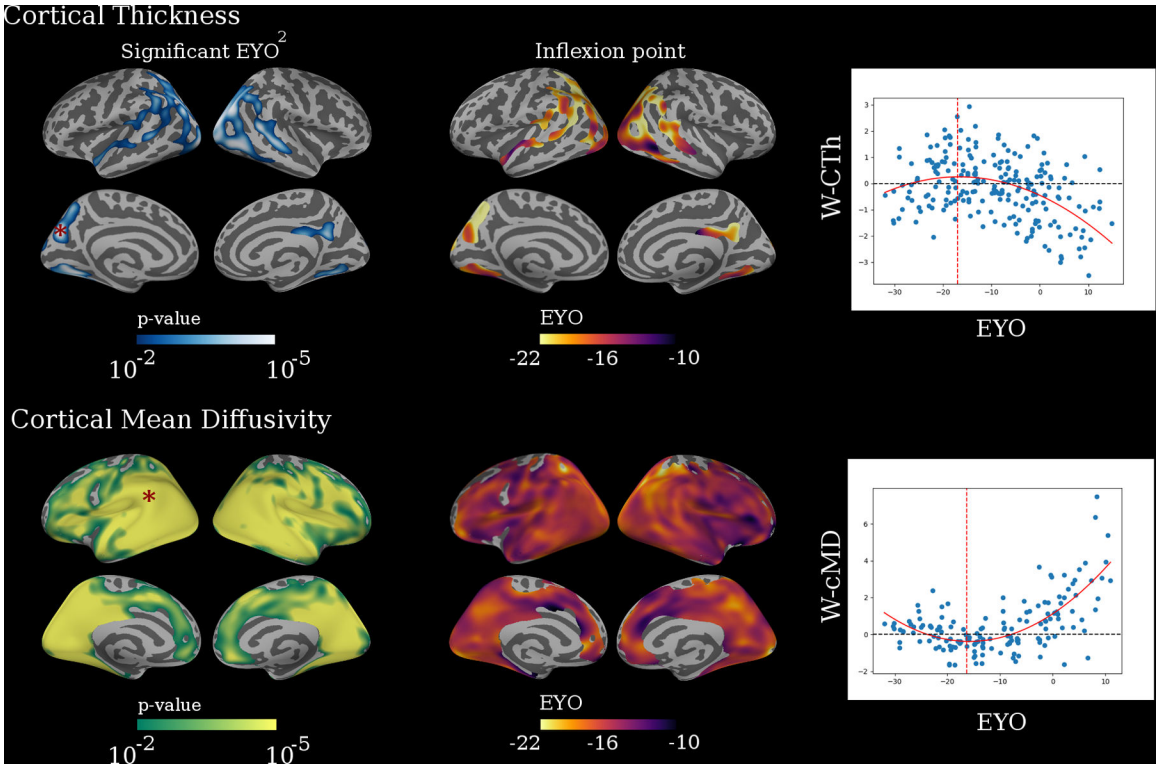

Figure 2. Brain regions showing a significant quadratic association with estimated years to symptom onset in mutation carriers.

Left panel shows the significant clusters for the association between the normalized cortical thickness (W-CTh; top row) and the normalized cortical mean diffusivity (W-MD; lower row) and the squared of estimated years of onset in mutation carriers participants. The middle panels show the inflection points for the W-CTh and W-MD (ie. the EYO at which W-CTh change from increasing to decreasing (top row) and where the W-MD change from decreasing to increasing (lower row). The right panels show the scatter plots for the fitting of the second order polynomial in the most significant vertex of the cortical mantle (marked as *) for both W-CTh (top row) and W-cMD (lower row). EYO = Estimated years to symptoms onset; W-CTh = Normalized cortical thickness; W-cMD = Normalized cortical mean diffusivity

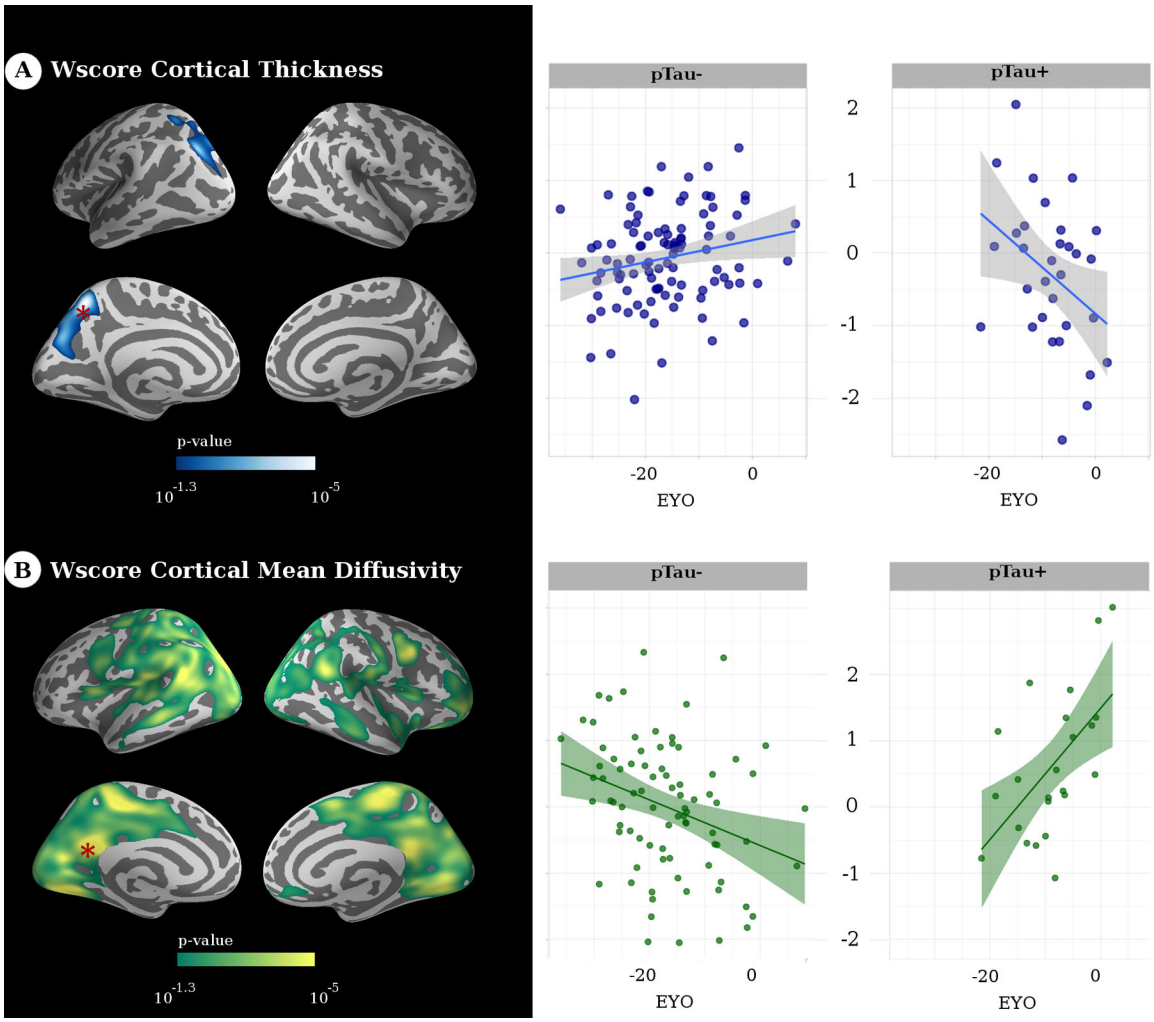

Figure 3. Interaction analyses between estimated years to symptom onset and CSF pTau positivity status on cortical thickness and cortical mean diffusivity.

Left panel: Brain regions with a significant interaction for both cortical thickness (top row) and cortical mean diffusivity (bottom row). Right panel: scatter plots for the interaction analyses in cortical thickness (upper right panel) and cortical mean diffusivity (lower right panel) in the most significant vertex for each interaction analysis (marked as red *). We only show those clusters that survived multiple comparisons correction. EYO = Estimated years to symptoms onset.

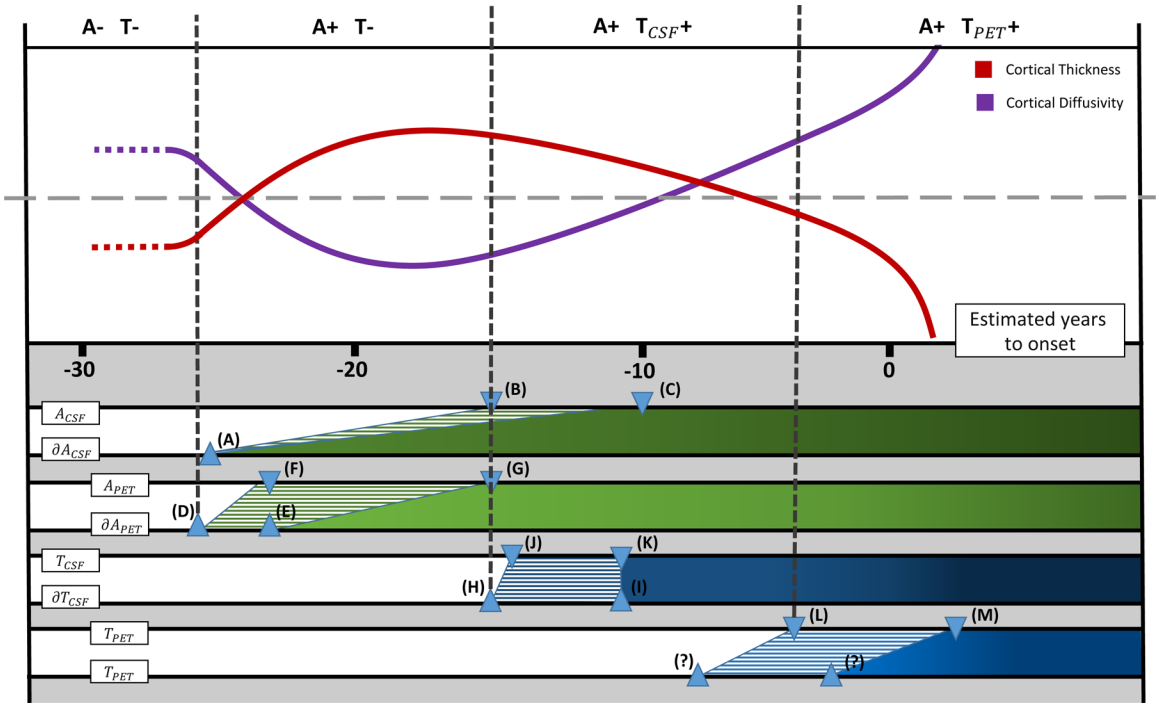

Figure 4. Hypothetical model of cortical thickness and cortical diffusivity changes in the presymptomatic phase of autosomal dominant Alzheimeŕs disease.

Top: Summary of MRI findings reported in the present study for cortical thickness (red) and cortical diffusivity (purple) Bottom: Previously reported time-points of pathophysiological biomarker changes. The ordering of the biomarkers correspond to: CSF amyloid levels, cross-sectional and rate of change (A_{CSF} and δA_{CSF}, respectively); amyloid PET, cross-sectional and rate of change (A_{PET} and δA_{PET}, respectively); CSF pTau levels, crossectional and rate of change (T_{CSF} and δT_{CSF}, respectively); and Tau PET, crossectional and rate of change (T_{PET} and δT_{PET}, respectively; the later hypothetical*). The letters refer to the different studies which report the estimated years to symptom onset at which these changes occur: (A) McDade et al 2018, (B) Bateman et al 2012, (C) McDade et al 2018, (D) McDade et al 2018, (E) Gordon et al 2018, (F) McDade et al 2018, (G) Bateman et al 2012, (H) Llibre-Guerra et al 2019, (I) Llibre-Guerra et al 2019, (J) Bateman et al 2012, (K) McDade et al 2018, (L) Quiroz et al 2018 and (M) Gordon et al 2019. *As there are no published longitudinal studies using Tau PET in autosomal dominant Alzheimeŕs disease, (?) refers to unknown event time-point of Tau PET longitudinal changes. Shaded color-lines reflect uncertainty of biomarker positivity due to discrepancies in the literature.

Table 1.
Demographics and clinical data of the participants.

N/A= Not applicable; DWI=Diffusion Weighted Imaging; *PSEN1*= Presenilin1; *PSEN2*=Presenilin2; *APP*=Amyloid Precursor Protein; EYO= Estimated Years to symptoms Onset; CDR=Clinical Dementia Rating

	Non-Carriers	Mutation Carriers
N (% DTI)	166 (74.7)	223 (70.4)
Asymptomatic (%)	N/A	68.1
Age (median, IQR)	36.74 [30.15 – 46.46]	36.48 [30.31 – 46.52]
Female (%)	57.2	54.7
Family Mutation *PSEN1/PSEN2/APP* (%)	65 / 12 / 23	72 / 9 / 17
EYO (median, IQR)	−10.41 [−19.1 – −2.5]	−9.13 [−18.56 – −1.31]
CDR (median, IQR)	0·0 [0 – 0]	0 [0 – 0.5]
CSF pTau pg/ml (median, IQR)	26.76 [21.9 – 34.22]	44.48 [31.1 – 83.5]